

Aggregation-Induced Emission of Tetraphenylethene–Hexaphenylbenzene Adducts: Effects of Twisting Amplitude and Steric Hindrance on Light Emission of Nonplanar Fluorogens

Rongrong Hu,^[a] Jacky W. Y. Lam,^[a] Yi Liu,^[a] Xiaoa Zhang,^[a] and Ben Zhong Tang*^[a, b]

Abstract: A series of nonplanar tetraphenylethene (TPE)–hexaphenylbenzene (HPB) adducts was designed and synthesized by Diels–Alder reaction of the acetylene precursors and tetraphenylcyclopentadienone. All of the adducts showed aggregation-induced emission features. The twisting amplitude and steric hindrance of the TPE and HPB units were found to play a crucial role in their fluorescence behaviors in the aggregated state.

Keywords: aggregation • cycloaddition • fluorescence • luminescence • steric hindrance

Introduction

Organic luminophores have attracted considerable interest for their potential device, sensing, and imaging applications.^[1] Many conventional fluorophores exhibit high fluorescence efficiency in solution but suffer an aggregation-caused quenching (ACQ) effect in the condensed phase, which prevents them from finding real-world applications in an engineering form.^[2] Many studies have been carried out since the 1930s to investigate the aggregation effect on the optical properties of organic dyes.^[3] In 2001, we observed a phenomenon of aggregation-induced emission (AIE) in some propeller-like molecules, such as tetraphenylethene (TPE) and hexaphenylsilole. These luminogens are nonemissive when molecularly dissolved in their good solvents, such as toluene, THF, and chloroform, but become highly luminescent in the aggregated state.^[4] We have considered a number of possible mechanistic pathways, including conformational planarization, J-aggregate formation, hydrophobic effect, *Z/E* isomerization, and twisted intramolecular charge transfer, as causes for the AIE effect but none of them was fully supported by the experimental results.^[5] Fundamental physics teaches that any molecular motions consume energy.

In solution, the active intramolecular rotation of the phenyl rings of TPE, for example, serves as a relaxation channel for the excitons to deactivate. In the aggregated state, such motion is restricted due to the physical constraint, which blocks the nonradiative pathway and activates radiative decay.^[6] We thus hypothesized that the restriction of intramolecular rotation is the cause of the AIE phenomenon. Thanks to the research enthusiasm of scientists, many AIE luminogens with different emission colors have been prepared and have found an array of high-tech applications as chemosensors, bioprobes, solid-state emitters for optical devices, and so forth.^[7]

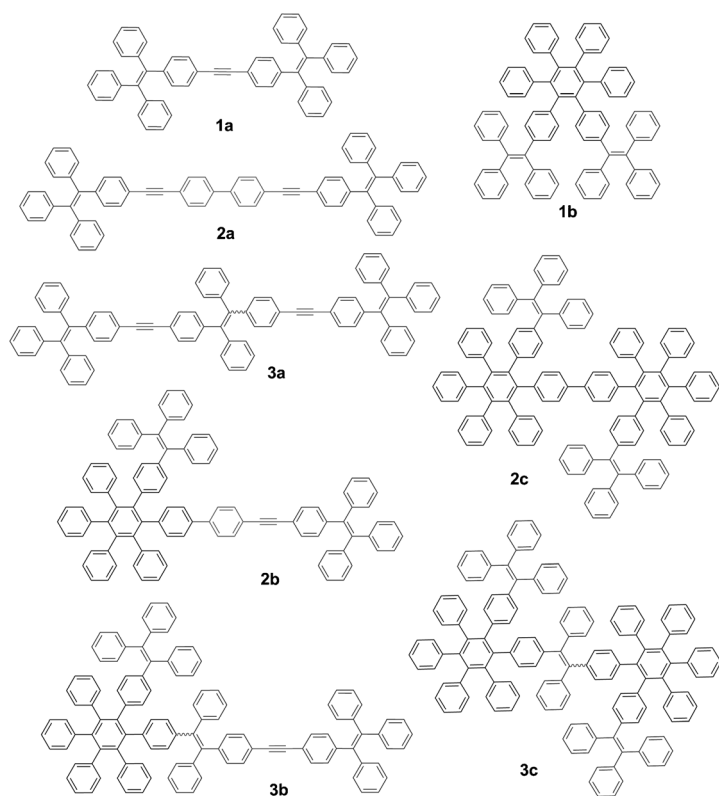
The conformational planarity and structural rigidity are found to play key roles in determining whether a luminogen exhibits AIE activity.^[8] Little effort, however, has been placed on studying how the twisting amplitude of the rotors affects the emission behaviors of nonplanar AIE luminogens. Hexaphenylbenzene (HPB) is an attractive building block for the construction of materials with novel properties because of its ready availability and facile modification.^[9] Similar to TPE, HPB is propeller-like in shape, which imparts large internal molecular free volume^[10] and impedes π – π stacking in the solid state, as demonstrated by the crystal structures of its derivatives.^[11] Unlike TPE, the peripheral phenyl rings in HPB cannot rotate freely due to the severe steric repulsion. Thus, it is an ideal compound, along with TPE, to investigate the effect of rotational freedom on the AIE process.

Attachment of HPB to traditional luminophores has solved their ACQ problem in the condensed phase, and the bulky, nonplanar structure of HPB prevents the formation of detrimental species such as excimers by intermolecular interactions.^[12] However, its effect in the AIE system remains less explored. What will be the consequence if HPB units are incorporated into the AIE systems? Tetrakis(pentaphenylphenyl)ethylene has been reported to show a higher fluorescence quantum yield ($\Phi_F=13\%$) than TPE ($\Phi_F=0.24\%$)^[13] in CH_2Cl_2 , presumably due to the steric

[a] Dr. R. Hu, Dr. J. W. Y. Lam, Y. Liu, X. Zhang, Prof. B. Z. Tang
The Hong Kong University of Science & Technology
Shenzhen Research Institute, Department of Chemistry
State Key Laboratory of Molecular Neuroscience
Institute of Molecular Functional Materials and
Division of Biomedical Engineering
The Hong Kong University of Science & Technology (HKUST)
Clear Water Bay, Kowloon, Hong Kong (P.R. China)
E-mail: tangbenz@ust.hk

[b] Prof. B. Z. Tang
Guangdong Innovative Research Team
SCUT–HKUST Joint Research Laboratory
State Key Laboratory of Luminescent Materials and Devices
South China University of Technology (SCUT)
Guang Zhou 51064 (P.R. China)

Supporting information for this article is available on the WWW under <http://dx.doi.org/10.1002/chem.201203840>.



Scheme 1. Chemical structures of **1a–3c**.

bulkiness of the HPB unit, which hampers the intramolecular rotations and thereby reduces the nonradiative decay of the excited state. In this work, we designed a series of non-planar luminogenic molecules constructed from TPE and HPB building blocks and investigated how the twisted structures of TPE and HPB affect the fluorescence of the resulting hybrid molecules in the solution and aggregated states (Scheme 1).

Results and Discussion

The TPE–HPB adducts were prepared according to the synthetic routes shown in Scheme 2. TPE-containing precursors **4**, **5**, and **3a** were prepared according to the previously published procedures.^[14] Palladium-catalyzed Sonogashira coupling of **4** and **5** afforded **1a**, which was transformed into **1b** by a Diels–Alder reaction with tetraphenylcyclopentadienone **6**. On the other hand, diyne **9** was obtained by a coupling reaction of **7** with trimethylsilylacetylene followed by base-catalyzed hydrolysis in THF. Under the same experimental procedures, **2a** was prepared from **9** and an excess amount of **4**. Diels–Alder reaction of **6** with **2a** or **3a** produced **2b** or **3b** with one HPB unit and one unreacted ethynyl group and **2c** or **3c** with two HPB units.

The structures of the intermediates and products were characterized by standard spectroscopic methods with satisfactory results (see the Experimental Section for details).

For example, the high-resolution mass spectra of **1b–3b**, **2c**, and **3c** give M^+ peaks at m/z 1042.4562 (**1b**), 1219.8142 (**2b**), 1575.6741 (**2c**), 1396.9825 (**3b**), and 1752.7534 (**3c**) (Figures S1–S7 in the Supporting Information), which are in good agreement with the calculated values. The $^1\text{H NMR}$ analysis provides more detailed structural information. The biphenyl protons of **2a**, for example, resonate at $\delta = 7.56$ ppm, which shifts to $\delta = 7.52$ ppm in the spectrum of **2b** (Figure 1). The broad multiplet observed at $\delta = 6.82$ ppm in **2b** is associated with the resonances of the newly formed HPB protons. Three peaks related to the absorptions of the phenyl protons shared by the HPB and TPE or biphenyl units are found at $\delta = 6.70$, 6.59, and 6.55 ppm, thus revealing that only half of the triple bonds of **2a** are converted to HPB units in **2b**. In **2c**, no peak was observed at $\delta = 7.56$ ppm and the resonances at $\delta = 6.82$, 6.67, 6.61, and 6.52 ppm are intensified, which suggests completeness of the Diels–Alder reaction. Similar phenomena are observed in the $^1\text{H NMR}$ spectra of **1a**, **1b**, and **3a–3c** (Figures S8 and S9 in the Supporting Information).

Although they are constructed from benzene rings, **1a–3c** dissolve readily in common organic solvents, such as toluene, chloroform, and THF, thanks to the twisted TPE and

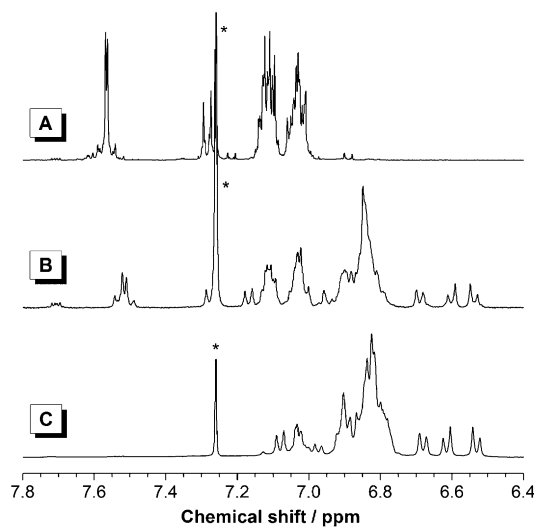
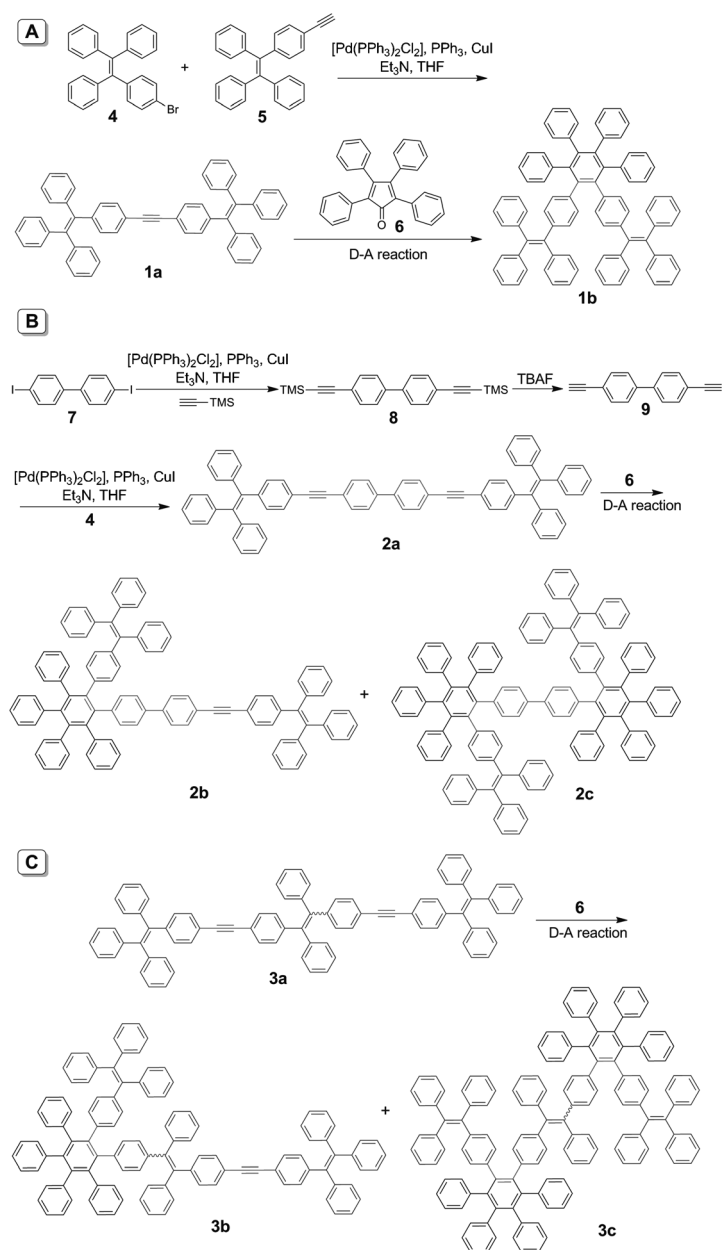


Figure 1. $^1\text{H NMR}$ spectra of A) **2a**, B) **2b**, and C) **2c** in $[\text{D}_6]$ chloroform. The solvent peaks are marked with asterisks.

HPB units, which endow large intermolecular distance and generate large free volume to accommodate more solvent molecules. The HPB–TPE adducts are also anticipated to show high resistance to thermolysis owing to the presence of numerous aromatic rings.^[15] Indeed, they enjoy high thermal stability, showing 5% weight loss at temperatures up to 460 °C under nitrogen and 422 °C in air (Figure 2 and Figures S10 and S11 in the Supporting Information). The high residual yield up to 40% is retained when these compounds are heated under nitrogen at 800 °C, implying their potential as ceramic materials.



Scheme 2. Synthetic routes to A) **1a** and **1b**, B) **2a–2c**, and C) **3b** and **3c**. D-A = Diels–Alder, TMS = trimethylsilyl, TBAF = tetrabutylammonium fluoride.

The absorption spectra of **1a–3c** as dilute solutions in THF are depicted in Figure 3. The spectra of **1a–3a** show peaks at 345, 353, and 352 nm, respectively (Figure 3 and Table 1). However, their adducts, **1b–3b**, absorb at shorter wavelengths of 331, 321, and 334 nm, respectively, due to the steric effect of the HPB unit. Compounds **2c** and **3c** carry two HPB units in one molecule, and they absorb at 310 and 324 nm, respectively, which are approximately 10 nm blueshifted from those of **2b** and **3b**. These results nicely demonstrate that the electronic transitions of the luminogens are sensitive to their molecular structures, thereby offering the opportunity to modulate their properties by mo-

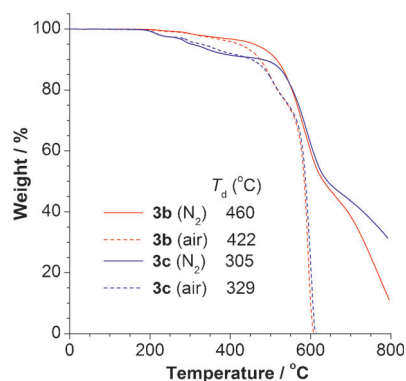


Figure 2. Thermogravimetric analysis (TGA) thermograms of **3b** and **3c** recorded under nitrogen and in air at a heating rate of $10^{\circ}\text{C min}^{-1}$. T_d = decompose temperature.

Table 1. Optical properties of **1a–3c**.^[a]

| Luminogen | λ_{ab} [nm] | λ_{em} [nm] | α_{AIE} | Φ_{solid} [%] |
|--------------------------|----------------------------|----------------------------|-----------------------|---------------------------|
| 1a | 345 | 484 | 479 | 87 |
| 1b | 331 | 480 | 204 | 48 |
| 2a | 353 | 482 | 269 | 63 |
| 2b | 321 | 477 | 204 | 21 |
| 2c | 310 | 462 | 18 | 10 |
| 3a ^[b] | 352 | 501 | 115 | 74 |
| 3b | 334 | 487 | 137 | 70 |
| 3c | 324 | 474 | 88 | 75 |

[a] Abbreviations: λ_{ab} = absorption maximum in THF (10 μM), λ_{em} = emission maximum in THF/water mixture (1:9, v/v), $\alpha_{\text{AIE}} = I_{\text{THF/water}}(1:9, \text{v/v})/I_{\text{THF}}$, Φ_{solid} = solid-state fluorescence quantum yield. [b] Data taken from ref. [10a].

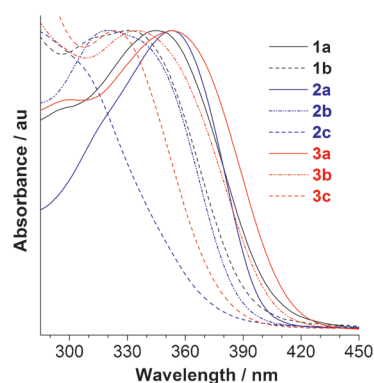


Figure 3. Normalized absorption spectra of **1a–3c** in THF. Solution concentration: 10 μM .

lecular engineering endeavors. The absorption of AIE luminogens is normally not affected by aggregate formation, as studied in our previous work.^[16] A similar observation was also made for the compounds studied herein. For example, no significant redshift in the absorption maximum was observed in the UV spectra of **1b** in THF/water mixtures with different amounts of water (Figure S12 in the Supporting Information). Level-off tails are seen in the visible spectral

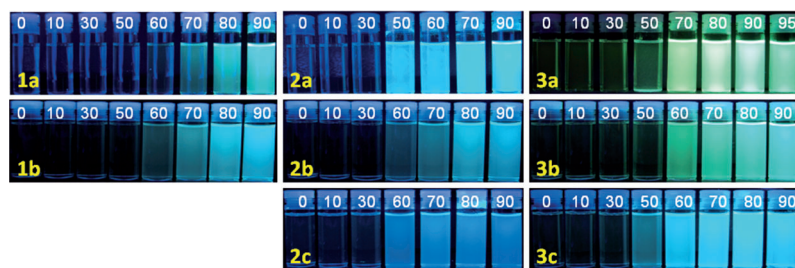


Figure 4. Photographs of **1a–3c** in THF/water mixtures with different water fractions (f_w) taken under UV illumination. Solution concentration: $10 \mu\text{M}$; percentage water is marked above each image.

region, which are attributed to the light-scattering effect of the nanoparticles.

All the molecules are AIE active, as suggested by the fluorescence images of their solutions in THF and THF/water mixtures (Figure 4). For example, the solution of **1a** in THF emits no light under UV illumination. Addition of water, a poor solvent of **1a**, to the solution aggregates its molecules and enhances its emission. The emission remains weak in aqueous mixtures with low water fractions ($\leq 70\%$) but becomes stronger when more water is added. Similar results were found with other compounds. Some luminogens become emissive in the presence of a small amount of water ($\approx 50\%$), presumably due to their comparatively lower solubility in the aqueous mixture.

In addition to visual observations, the emission behaviors of **1a–3c** in THF/water mixtures were studied by spectrofluorometry. As shown in Figure 5 A, compound **1b** is practi-

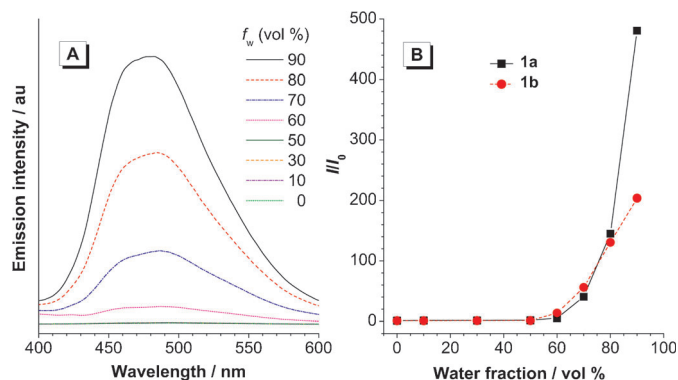


Figure 5. A) Photoluminescence (PL) spectra of **1b** in THF/water mixtures with different water fractions (f_w). B) Plots of I/I_0 values versus the compositions of aqueous mixtures of **1a** and **1b**. Solution concentration: $10 \mu\text{M}$; excitation wavelength: 345 (**1a**) and 331 nm (**1b**).

cally nonemissive in THF. When the water fraction in the solvent mixture is 60%, an emission peak emerges at 480 nm, the intensity of which is enhanced, without causing any spectral profile change, by further increasing the water solvent fraction. From the solution in THF to nanoaggregates in a 90% aqueous mixture, the emission intensity rises by 204-fold (Figure 5B). Under the same circumstances, the emission enhancement, or the α_{AIE} value, of **1a** (479) is

much higher than that of **1b** (Figure S13 in the Supporting Information); α_{AIE} is the AIE factor defined by the following equation: $\alpha_{\text{AIE}} = I_{\text{THF/water (1:9, v/v)}} / I_{\text{THF}}$. Similarly, compound **2a** emits no light in THF, but its nanoaggregates in a 90% aqueous mixture emit intensely at 482 nm with a 269-fold higher intensity (Figure 6A). Lumino-

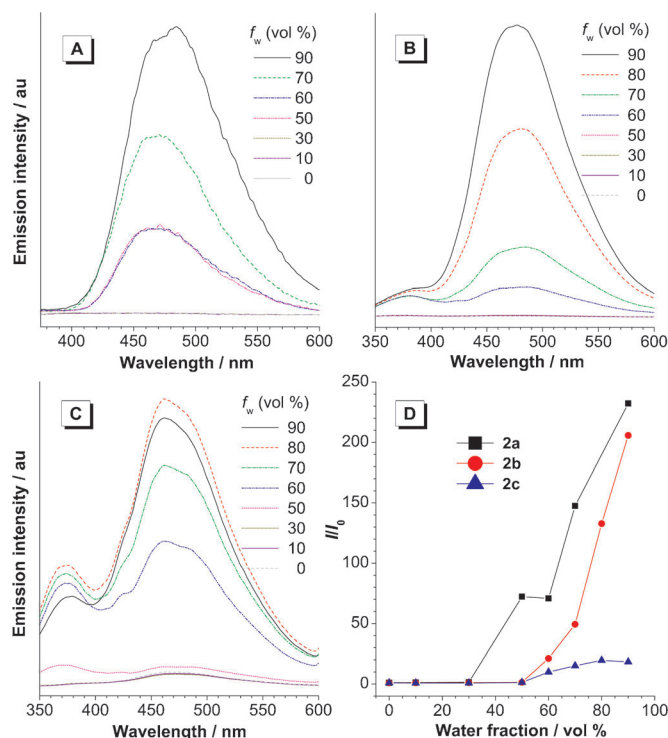


Figure 6. Emission spectra of A) **2a**, B) **2b**, and C) **2c** in THF/water mixtures with different water fractions (f_w). D) Plots of I/I_0 values versus the compositions of aqueous mixtures of **2a–2c**. Solution concentration: $10 \mu\text{M}$; excitation wavelength: 353 (**2a**), 321 (**2b**), and 310 nm (**2c**).

gen **2b**, with one HPB unit, on the other hand, fluoresces at 477 nm in the aggregated state with an α_{AIE} value (204) close to that of **2a** (Figure 6B and 6D). On the other hand, compound **2c** contains two HPB units and shows a broad emission peak at 462 nm in THF although the intensity is weak (Figure 6C). The emission intensity starts to rise when water is added to the solution in THF and reaches its maximum value for an 80% aqueous mixture, with a much smaller α_{AIE} value of 18. A similar trend was observed in the photoluminescence (PL) spectra of **3a–3c** (Figure 7 and Figure S14 in the Supporting Information).

We also investigated the PL of **1a–3c** in the solid state. All the solid powders of **1a–3c** show strong light emissions at wavelengths similar to those of their nanoaggregates in THF/water suspensions (Figure S15 in the Supporting Infor-

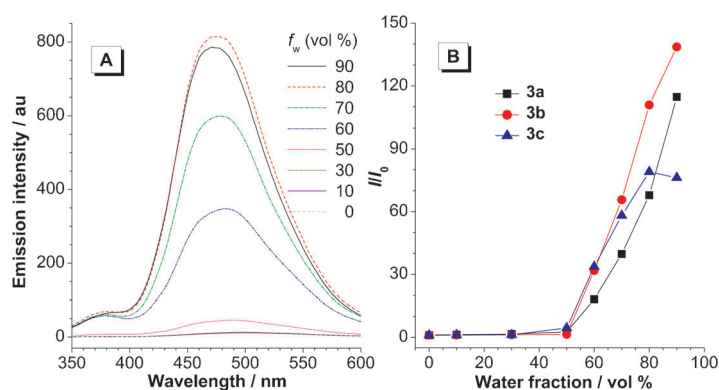


Figure 7. A) PL spectra of **3c** in THF/water mixtures with different water fractions (f_w). B) Plots of I/I_0 values versus the compositions of aqueous mixtures of **3a–3c**. Solution concentration: 10 μM ; excitation wavelength: 352 (**3a**), 334 (**3b**), and 324 nm (**3c**).

mation). We determined their fluorescence quantum yields (Φ_{FS}) by a calibrated integrating sphere (Table 1) and high Φ_{FS} values up to 87% were deduced from the measurements, manifesting their AIE features. The Φ_{FS} values of **1a–3a** are higher than those of **1b–3b**, **2c**, and **3c**. This suggests that the incorporation of the HPB unit into AIE luminogens is harmful to the emission of the resulting adducts.

Why is there such a Φ_{FS} difference, considering that both TPE and HPB units take a twisted, propeller-like structure? The four phenyl rings in TPE can undergo free rotation with a large twisting amplitude. However, the rotation of the phenyl rings in HPB is more difficult because of the severe steric hindrance from the neighborhood. Hence, TPE shows no discernible emission peak in solution, whereas HPB emits a weak PL peak at 334 nm in THF (Figure 8). In an 80% aqueous solvent mixture, the emission from HPB is increased by 12-fold, accompanied by a 5 nm blueshift in the emission maximum, thereby displaying a phenomenon of aggregation-enhanced emission. The HPB unit plays dual roles in the photophysical processes of **1b–3c**. Its bulky size restricts the intramolecular rotation of the phenyl rings in sol-

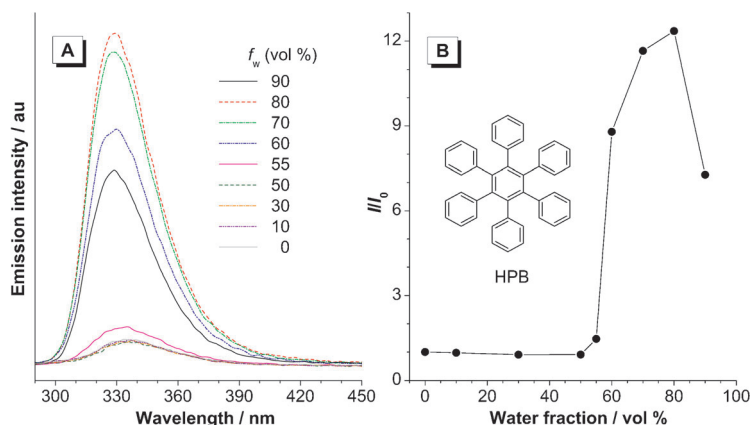


Figure 8. A) Emission spectra of HPB in THF/water mixtures. B) Plot of I/I_0 values versus the compositions of aqueous mixtures of HPB. Concentration: 10 μM ; excitation wavelength: 272 nm.

ution, thus reducing the energy loss of the excitons through nonradiative relaxation channels. Furthermore, it impedes the close packing of the molecules in the aggregated state, thus reducing the formation of species that are detrimental to the light emission. On the other hand, the increment of the intermolecular distance generates more free volume, which allows the phenyl rings to rotate to a certain extent. This weakens the light emission in the aggregated state and hence decreases the α_{AIE} value.

To gain a quantitative characterization of the phenyl ring rotations, single-crystal structures of TPE and HPB,^[17] as well as their optimized structures obtained by theoretical calculations, are compared in Figures 9 and 10. In TPE, the

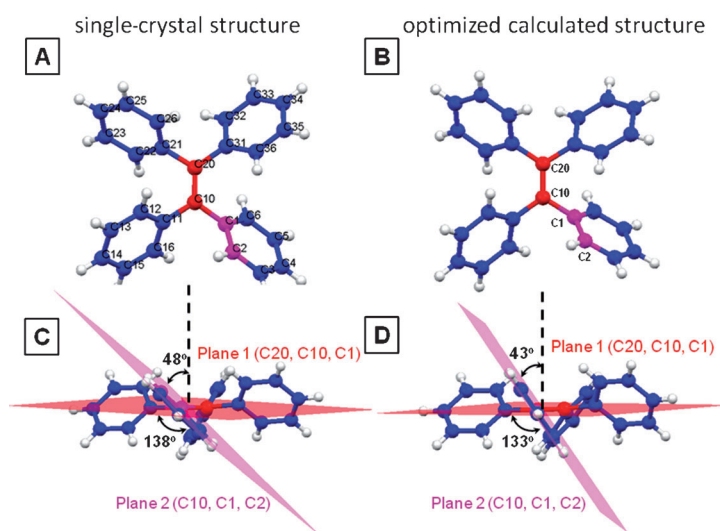


Figure 9. A,C) Single-crystal structure and B,D) optimized calculated structure of TPE. CCDC-633293 contains the supplementary crystallographic data for this paper. These data can be obtained free of charge from The Cambridge Crystallographic Data Centre via www.ccdc.cam.ac.uk/data_request/cif.

four peripheral phenyl rings are twisted out of the central double-bond plane. The dihedral angle of C20–C10–C1–C2 is 138°, as suggested by the single-crystal structure. This indicates that the phenyl ring in plane 2 deviates from the perpendicular position of plane 1 by 48° where the central double bond lies (Figure 9C). A similar value (43°) was obtained from theoretical calculations (Figure 9B and 9D). In HPB, the peripheral phenyl rings are almost perpendicular to the central benzene ring. Through the single-crystal structure, the dihedral angle of C1–C2–C13–C14 is 102°, from which a twisting angle of 12° is derived. This value is much smaller than that in TPE, which is suggestive of a smaller twisting amplitude of the phenyl rings in HPB. Although the optimized structure reveals a higher twisting angle of 22°, such a value is still small when compared with TPE.

The potential energy curves along the dihedral angle of the ground state for isolated TPE and HPB molecules are calculated and shown in Figure 11. The energy barrier of phenyl-ring rotation in TPE is about 8 kcal mol^{−1}, whereas

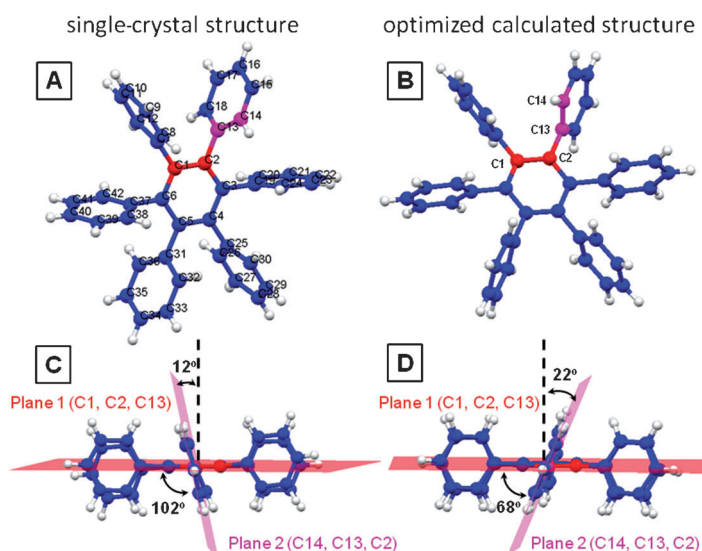


Figure 10. A,C) Single-crystal structure and B,D) optimized calculated structure of HPB. CCDC-177146 contains the supplementary crystallographic data for this paper. These data can be obtained free of charge from The Cambridge Crystallographic Data Centre via www.ccdc.cam.ac.uk/data_request/cif.

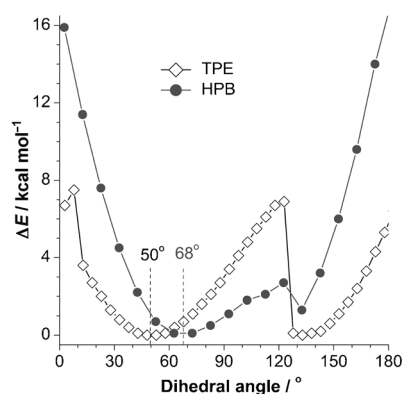


Figure 11. Potential energy curves along the dihedral angle of the ground state for isolated TPE (C20-C10-C1-C2) and HPB (C1-C2-C13-C14) molecules.

the value in HPB is doubled, which demonstrates that the rotation of the phenyl rings in HPB is more difficult. Moreover, the dihedral angle for minimum energy is 50° for TPE and 68° for HPB, from which twisting angles of 40 and 22° are deduced for TPE and HPB, respectively. All these results show the higher twisting amplitude in TPE.

Conclusion

A series of luminogenic materials has been designed and synthesized from TPE and HPB building blocks. They are all AIE active with high solid-state fluorescence quantum yields up to 87%. The twisting amplitude and steric effects are found to be crucial for the AIE behavior in nonplanar

fluorogens. Such a structure–property relationship will deepen our mechanistic understanding of this new phenomenon and guide the future design of materials.

Experimental Section

Materials: Tetrahydrofuran (THF) and toluene were distilled under normal pressure from sodium benzophenone ketyl under nitrogen immediately prior to use. Dichlorobis(triphenylphosphine)palladium(II) ($[\text{Pd}(\text{PPh}_3)_2\text{Cl}_2]$), copper(I) iodide (CuI), triphenylphosphine (PPh_3), tetrabutylammonium fluoride (TBAF), trimethylsilylacetylene, triethylamine (Et_3N), 2,3,4,5-tetraphenylcyclopentadienone (**6**), and other chemicals and solvents were all purchased from Aldrich and used as received without further purification. 1-(4-Bromophenyl)triphenylethene (**4**), 1-(4-ethynylphenyl)triphenylethene (**5**), and 1,2-bis[4-(2-(4-triphenylvinyl)phenyl)ethynyl]phenyl-1,2-diphenylethene (**3a**) were prepared according to the previously published procedures.^[14]

Instruments: ^1H NMR spectra were measured on a Bruker ARX 400 NMR spectrometer with CDCl_3 or CD_2Cl_2 as solvent and tetramethylsilane (TMS; $\delta = 0$ ppm) as internal standard. IR spectra were recorded on a Perkin–Elmer 16 PC FTIR spectrophotometer. Thermogravimetric analysis (TGA) was carried out under nitrogen or in air on a Perkin–Elmer TGA 7 analyzer at a heating rate of $10^\circ\text{C}\text{min}^{-1}$. UV/Vis absorption spectra were measured on a Milton Roy Spectronic 3000 array spectrophotometer. Photoluminescence (PL) spectra were recorded on a Perkin–Elmer LS 55 spectrofluorometer. High-resolution mass spectra were recorded on a GCT premier CAB048 mass spectrometer operating in MALDI-TOF mode. The ground-state geometries of TPE and HPB were optimized by density functional theory (DFT). The DFT calculations were carried out by using the B3LYP functionals with the 6-31g-(d,p) basis set.^[18]

Preparation of aggregates: Stock solutions of the molecules in THF were prepared with a concentration of 0.1 mM. An aliquot (1 mL) of this stock solution was transferred to a volumetric flask (10 mL). After adding an appropriate amount of THF, water was added dropwise under vigorous stirring to furnish a 10 μM solution in a THF/water mixture with a specific water fraction (f_w). The water content was varied in the range of 0–90 vol%. Absorption and emission spectra of the resulting solutions and aggregates were measured immediately after sample preparation.

Synthesis and characterization: Compounds **1a–3c** were synthesized according to the synthetic routes shown in Scheme 2. Detailed experimental procedures are given below. Although the Diels–Alder reaction is known as a quantitative reaction in many cases, the small polarity difference between the reactants **1a–3a** and products **1b–3b**, **2c**, and **3c**, as well as their poor solubility in nonpolar solvents such as hexane, lowered the yield of isolated products significantly.

4,4'-Bis(2-trimethylsilylethynyl)biphenyl (8): Compound **7** (5.00 g, 12.3 mmol), $[\text{Pd}(\text{PPh}_3)_2\text{Cl}_2]$ (0.43 g, 0.62 mmol), CuI (0.12 g, 0.62 mmol), PPh_3 (0.10 g, 0.37 mmol), and a solvent mixture of THF/ Et_3N (100/50 mL) were added to a two-necked round-bottom flask (250 mL) in the atmosphere of nitrogen. After the catalysts were completely dissolved, (trimethylsilyl)acetylene (5.22 mL, 36.9 mmol) was injected into the flask and the mixture was stirred at 70°C for 24 h. The formed solid was removed by filtration and washed with diethyl ether. The solvent was removed under reduced pressure and the crude product was purified on a silica-gel column with hexane as eluent. A pale-brown solid (**8**) was obtained in 96% yield. ^1H NMR (400 MHz, CDCl_3): δ (TMS) = 7.53 (s, 8H), 0.27 ppm (s, 18H); IR (KBr): $\tilde{\nu}$ = 3036, 2956, 2899, 2157 ($\text{C}\equiv\text{C}$ stretching), 1918, 1488, 1399, 1253, 1242, 1220, 1113, 1004, 847, 823, 758, 697, 646, 543 cm^{-1} ; HRMS (MALDI-TOF): m/z calcd for $\text{C}_{22}\text{H}_{26}\text{Si}_2$: 346.1573 [M]⁺; found: 346.1252.

4,4'-Diethynylbiphenyl (9): A solution of **8** in THF (120 mL, 3.80 g, 11.0 mmol) and TBAF (1 M; 44 mL) were placed into a round-bottom flask (250 mL). After stirring for 3 h, water (120 mL) was added and the mixture was then extracted three times with dichloromethane. The solu-

tion in CH_2Cl_2 was washed with twice brine and dried over anhydrous sodium sulfate. After filtration and solvent evaporation, the crude product was purified on a silica-gel column with petroleum ether as eluent. A light-yellow solid (**9**) was obtained in 89% yield. $^1\text{H NMR}$ (400 MHz, CD_2Cl_2): δ (TMS) = 7.56 (s, 8H), 3.14 ppm (s, 2H); IR (KBr), $\tilde{\nu}$ = 3467 (= C–H stretching), 3273, 3035, 2106 (C=C stretching), 1919, 1694, 1660, 1604, 1489, 1393, 1252, 1108, 1004, 857, 825, 678, 658, 647, 632, 565, 546, 513 cm^{-1} ; HRMS (MALDI-TOF): m/z calcd for $\text{C}_{16}\text{H}_{10}$: 202.0783 [M] $^+$; found: 202.0774.

4,4'-Bis(1,2,2-triphenylvinyl)diphenylacetylene (1a): A two-necked flask was charged with **4** (0.51 g, 1.24 mmol), **5** (0.40 g, 1.12 mmol), $[\text{Pd}(\text{PPh}_3)_2\text{Cl}_2]$ (16 mg, 0.02 mmol), PPh_3 (3 mg, 0.01 mmol), and CuI (4 mg, 0.02 mmol). The flask was degassed and filled with nitrogen. A mixture of THF (12 mL) and Et_3N (6 mL) was then added by syringe. The mixture was stirred at reflux for 24 h under nitrogen. The solution was allowed to cool to room temperature and washed with saturated aqueous NH_4Cl . The mixture was extracted with CH_2Cl_2 and washed with brine. The organic extracts were separated, combined, and dried over anhydrous MgSO_4 . After filtration and solvent removal under vacuum, the residue was purified by silica-gel column chromatography with petroleum ether as eluent. A yellow solid (**1a**) was isolated in 89% yield. $^1\text{H NMR}$ (400 MHz, CDCl_3): δ (TMS) = 7.21 (d, J = 8 Hz, 4H), 7.10 (m, 18H), 7.02 (m, 12H), 6.98 ppm (d, J = 8 Hz, 4H); IR (KBr), $\tilde{\nu}$ = 3056, 3021, 1598, 1491, 1441, 1075, 1029, 853, 824, 748, 699 cm^{-1} ; HRMS (MALDI-TOF): m/z calcd for $\text{C}_{54}\text{H}_{38}$: 686.2974 [M] $^+$; found: 686.2964.

1,2-Bis[4-(1,2,2-triphenylvinyl)phenyl]-3,4,5,6-tetraphenylbenzene (1b): Compound **1a** (0.25 g, 0.36 mmol), **6** (0.17 g, 0.44 mmol), and diphenyl ether (5 mL) were added to a round-bottom flask. After heating at reflux for 48 h under nitrogen, the solution was cooled to room temperature and diluted with ethanol. The precipitate was separated by filtration and washed with ethanol. The crude product was purified by silica-gel column chromatography with petroleum ether as eluent. A yellow solid was isolated (**1b**) in 32% yield. $^1\text{H NMR}$ (400 MHz, CDCl_3): δ (TMS) = 7.34 (t, J = 8.0 Hz, 2H), 6.99 (m, 50H), 6.57 (d, J = 8.4 Hz, 2H), 6.50 ppm (d, J = 8.0 Hz, 2H); IR (KBr), $\tilde{\nu}$ = 3056, 3025, 2924, 1725, 1583, 1487, 1442, 1236, 1073, 1023, 750, 699 cm^{-1} ; HRMS (MALDI-TOF): m/z calcd for $\text{C}_{82}\text{H}_{58}$: 1042.4539 [M] $^+$; found: 1042.4562.

4,4'-Bis[2-[4-(1,2,2-triphenylvinyl)phenyl]ethynyl]biphenyl (2a): A two-necked flask was charged with **9** (3.00 g, 7.29 mmol), **4** (0.49 g, 2.43 mmol), $[\text{Pd}(\text{PPh}_3)_2\text{Cl}_2]$ (136 mg, 0.19 mmol), PPh_3 (64 mg, 0.24 mmol), and CuI (28 mg, 0.14 mmol). The flask was degassed and filled with nitrogen. A mixture of THF (100 mL) and Et_3N (50 mL) was then added by syringe. After stirring at reflux for 24 h under nitrogen, the mixture was cooled to room temperature and washed with saturated aqueous NH_4Cl . The mixture was extracted with CH_2Cl_2 and washed with brine. The organic extracts were separated and dried over anhydrous MgSO_4 . After filtration and solvent evaporation under vacuum, the residue was purified by silica-gel column chromatography with petroleum ether as eluent to give **2a** as a yellow solid in 25% yield. $^1\text{H NMR}$ (400 MHz, CDCl_3): δ (TMS) = 7.56 (m, J = 2 Hz, 8H), 7.28 (m, J = 8.4 Hz, 4H), 7.11 (m, 18H), 7.03 ppm (m, 16H); IR (KBr), $\tilde{\nu}$ = 2925, 2856, 1509, 1491, 1462, 1443, 1378, 822, 700 cm^{-1} ; HRMS (MALDI-TOF): m/z calcd for $\text{C}_{68}\text{H}_{46}$: 862.3600 [M] $^+$; found: 862.3597.

Compounds 2b and 2c: Compound **2a** (0.30 g, 0.35 mmol), **6** (0.53 g, 1.39 mmol), and diphenyl ether (5 mL) were added to a round-bottom flask. After heating at reflux for 48 h under nitrogen, the solution was cooled to room temperature and diluted with ethanol. The precipitate was separated by filtration and washed with ethanol. The crude product was purified by silica-gel column chromatography with petroleum ether as eluent. Compounds **2b** and **2c** were obtained in 39 and 37% yield, respectively. **2b**: $^1\text{H NMR}$ (400 MHz, CDCl_3): δ (TMS) = 7.52 (m, 8H), 7.09 (m, 18H), 6.88 (m, 28H), 6.70 (d, J = 6.8 Hz, 4H), 6.59 (d, J = 8.4 Hz, 4H), 6.55 ppm (d, J = 8.4 Hz, 4H); IR (KBr), $\tilde{\nu}$ = 3026, 2925, 2347, 1730, 1600, 1493, 1443, 1270, 1073, 698 cm^{-1} ; HRMS (MALDI-TOF): m/z calcd for $\text{C}_{96}\text{H}_{66}$: 1218.5165 [M] $^+$; found: 1219.8142. **2c**: $^1\text{H NMR}$ (400 MHz, CDCl_3): δ (TMS) = 7.02 (m, 14H), 6.85 (m, 60H), 6.67 (d, J = 7.6 Hz, 4H), 6.61 (d, J = 8.0 Hz, 4H), 6.52 ppm (d, J = 8.4 Hz, 4H); IR (KBr), $\tilde{\nu}$ =

3025, 2959, 2927, 1600, 1494, 1443, 1074, 1029, 731, 697 cm^{-1} ; HRMS (MALDI-TOF): m/z calcd for $\text{C}_{124}\text{H}_{86}$: 1574.6730 [M] $^+$; found: 1574.6741.

Compounds 3b and 3c: Compound **3a** (0.30 g, 0.29 mmol), **6** (0.44 g, 1.15 mmol), and diphenyl ether (5 mL) were added to a round-bottom flask. After heating at reflux for 48 h under nitrogen, the mixture was cooled to room temperature and diluted with ethanol. The precipitate was separated by filtration and washed with ethanol. The crude product was purified by silica-gel column chromatography with petroleum ether as eluent. Compounds **3b** and **3c** were obtained in 21 and 44% yield, respectively. **3b**: $^1\text{H NMR}$ (400 MHz, CDCl_3): δ (TMS) = 7.20 (m, 4H), 7.06 (m, 36H), 6.86 (m, 28H), 6.56 (m, 4H), 6.51 ppm (m, 4H); IR (KBr), $\tilde{\nu}$ = 3441, 3055, 3026, 2959, 2927, 1945, 1884, 1802, 1727, 1600, 1493, 1443, 1262, 1074, 1029, 803, 751, 730, 698 cm^{-1} ; HRMS (MALDI-TOF): m/z calcd for $\text{C}_{110}\text{H}_{76}$: 1396.5947 [M] $^+$; found: 1396.9825. **3c**: $^1\text{H NMR}$ (400 MHz, CDCl_3): δ (TMS) = 7.08 (d, J = 8.4 Hz, 4H), 7.03 (m, 8H), 6.97 (d, J = 7.2 Hz, 4H), 6.90 (m, 16H), 6.82 (m, 52H), 6.68 (d, J = 7.2 Hz, 4H), 6.61 (d, J = 8.4 Hz, 4H), 6.53 ppm (d, J = 8.4 Hz, 4H); IR (KBr), $\tilde{\nu}$ = 3023, 1585, 1485, 1442, 1390, 1234, 1074, 1022, 750, 726, 697 cm^{-1} ; HRMS (MALDI-TOF): m/z calcd for $\text{C}_{138}\text{H}_{96}$: 1752.7512 [M] $^+$; found: 1752.7534.

Acknowledgements

We thank Luming Meng and Prof. Xuhui Huang for technical support on theoretical calculations. This work was partially supported by the National Basic Research Program of China (973 Program; 2013CB834701), the RPC and SRFI Grants of HKUST (RPC11SC09 and SRFI11SC03PG), the Research Grants Council of Hong Kong (HKUST2/CRF/10 and N_HKUST620/11), the Innovation and Technology Commission (ITCPD/17-9), and the University Grants Committee of HK (AoE/P-03/08). B.Z.T. is grateful for the support of the Guangdong Innovative Research Team Program (201101C0105067115).

- [1] a) S. W. Thomas III, G. D. Joly, T. M. Swager, *Chem. Rev.* **2007**, *107*, 1339–1386; b) S. H. Hwang, C. N. Moorefield, G. R. Newkome, *Chem. Soc. Rev.* **2008**, *37*, 2543–2557; c) Y. Shirota, H. Kageyama, *Chem. Rev.* **2007**, *107*, 953–1010.
- [2] a) B. M. Krasovitskii, B. M. Bolotin in *Organic Luminescent Materials*, VCH, Weinheim, **1988**; b) U. Lemmer, S. Heun, R. F. Mahrt, U. Scherf, M. Hopmeier, U. Siegler, E. O. Göbel, K. Müllen, H. Bässler, *Chem. Phys. Lett.* **1995**, *240*, 373–378; c) M. Grell, D. D. C. Bradley, G. Ungar, J. Hill, K. S. Whitehead, *Macromolecules* **1999**, *32*, 5810–5817; d) R. Jakubiak, C. J. Collison, W. C. Wan, L. Rothberg, *J. Phys. Chem. A* **1999**, *103*, 2394–2398.
- [3] a) E. E. Jelley, *Nature* **1936**, *138*, 1009–1010; b) G. Scheibe, *Angew. Chem.* **1937**, *50*, 212–219; c) E. E. Jelley, *Nature* **1937**, *139*, 631–632.
- [4] a) J. Luo, Z. Xie, J. W. Y. Lam, L. Cheng, H. Chen, C. Qiu, H. S. Kwok, X. Zhan, Y. Liu, D. Zhu, B. Z. Tang, *Chem. Commun.* **2001**, 1740–1741; b) B. Z. Tang, X. Zhan, G. Yu, P. P. S. Lee, Y. Liu, D. Zhu, *J. Mater. Chem.* **2001**, *11*, 2974–2978.
- [5] a) T. Morozumi, T. Anada, H. Nakamura, *J. Phys. Chem. B* **2001**, *105*, 2923–2931; b) A. Bajorek, J. Paczkowski, *Macromolecules* **1998**, *31*, 86–95; c) T. Soujanya, R. W. Fessenden, A. Samanta, *J. Phys. Chem.* **1996**, *100*, 3507–3512.
- [6] a) J. Chen, C. C. W. Law, J. W. Y. Lam, Y. Dong, S. M. F. Lo, I. D. Williams, D. Zhu, B. Z. Tang, *Chem. Mater.* **2003**, *15*, 1535–1546; b) Q. Peng, Y. Yi, Z. Shuai, J. Shao, *J. Am. Chem. Soc.* **2007**, *129*, 9333–9339; c) S. Yin, Q. Peng, Z. Shuai, W. Fang, Y. H. Wang, Y. Luo, *Phys. Rev. B* **2006**, *73*, 205409; d) X. Fan, J. Sun, F. Wang, Z. Chu, P. Wang, Y. Dong, R. Hu, B. Z. Tang, D. Zou, *Chem. Commun.* **2008**, 2989–2991; e) Z. Li, Y. Dong, B. Mi, Y. Tang, M. Haeussler, H. Tong, Y. Dong, J. W. Y. Lam, Y. Ren, H. H. Y. Sung, K. S. Wong, P. Gao, I. D. Williams, H. S. Kwok, B. Z. Tang, *J. Phys. Chem. B* **2005**, *109*, 10061–10066.
- [7] a) S. Sharafy, K. A. Muszkat, *J. Am. Chem. Soc.* **1971**, *93*, 4119–4125; b) Y. Hong, J. W. Y. Lam, B. Z. Tang, *Chem. Commun.* **2009**, 4332–4353; c) Z. Zhao, S. Chen, J. W. Y. Lam, P. Lu, Y. Zhong, K. S.

- Wong, H. S. Kwok, B. Z. Tang, *Chem. Commun.* **2010**, *46*, 2221–2223; d) B. K. An, S. H. Gihm, J. W. Chung, C. R. Park, S. K. Kwon, S. Y. Park, *J. Am. Chem. Soc.* **2009**, *131*, 3950–3957; e) M. C. Zhao, M. Wang, H. Liu, D. S. Liu, G. X. Zhang, D. Q. Zhang, D. B. Zhu, *Langmuir* **2009**, *25*, 676–678.
- [8] a) Y. Hong, J. W. Y. Lam, B. Z. Tang, *Chem. Soc. Rev.* **2011**, *40*, 5361–5388; b) M. Shimizu, H. Tatsumi, K. Mochida, K. Shimono, T. Hiyama, *Chem. Asian J.* **2009**, *4*, 1289–1297; c) R. Kabe, H. Nakanotani, T. Sakanoue, M. Yahiro, C. Adachi, *Adv. Mater.* **2009**, *21*, 4034–4038.
- [9] a) W. D. Watson, A. Fechtenkotter, K. Müllen, *Chem. Rev.* **2001**, *101*, 1267–1300; b) Z. Li, S. Ye, Y. Liu, G. Yu, W. Wu, J. Qin, Z. Li, *J. Phys. Chem. B* **2010**, *114*, 9101–9108; c) M. A. Keegstra, S. DeFeyter, F. C. DeSchryver, K. Müllen, *Angew. Chem.* **1996**, *108*, 830–833; *Angew. Chem. Int. Ed. Engl.* **1996**, *35*, 774–776; d) S. Watanabe, J. Kido, *Chem. Lett.* **2007**, *36*, 590–591; e) K. Kobayashi, N. Kobayashi, M. Ikuta, B. Therrien, S. Sakamoto, K. Yamaguchi, *J. Org. Chem.* **2005**, *70*, 749–752.
- [10] a) D. Gust, *J. Am. Chem. Soc.* **1977**, *99*, 6980–6982; b) T. M. Long, T. M. Swager, *Adv. Mater.* **2001**, *13*, 601–604.
- [11] S. Wang, W. J. Oldham, Jr., R. A. Hudack, G. C. Bazan, *J. Am. Chem. Soc.* **2000**, *122*, 5695–5709.
- [12] B. Valeur, *Molecular Fluorescence*, Wiley-VCH, Weinheim, **2002**.
- [13] a) V. S. Vyas, R. Rathore, *Chem. Commun.* **2010**, *46*, 1065–1067; b) Z. Zhao, S. Chen, J. W. Y. Lam, C. K. W. Jim, C. Y. K. Chan, Z. Wang, P. Lu, C. Deng, H. S. Kwok, Y. Ma, B. Z. Tang, *J. Phys. Chem. C* **2010**, *114*, 7963–7972; c) R. Rathore, C. L. Burns, S. A. Abdelwahed, *Org. Lett.* **2004**, *6*, 1689–1692; d) M. Banerjee, S. J. Emond, S. V. Lindeman, R. Rathore, *J. Org. Chem.* **2007**, *72*, 8054–8061.
- [14] a) R. Hu, J. L. Maldonado, M. Rodriguez, C. Deng, C. K. W. Jim, J. W. Y. Lam, M. M. F. Yuen, G. R. Ortiz, B. Z. Tang, *J. Mater. Chem.* **2012**, *22*, 232–240; b) R. Hu, J. W. Y. Lam, J. Liu, H. H. Y. Sung, I. D. Williams, Z. Yue, K. S. Wong, M. M. F. Yuen, B. Z. Tang, *Polym. Chem.* **2012**, *3*, 1481–1489.
- [15] a) P. Kundu, K. R. J. Thomas, J. T. Lin, Y. T. Tao, C. H. Chien, *Adv. Funct. Mater.* **2003**, *13*, 445–452; b) J. Y. Shen, C. Y. Lee, T. H. Huang, J. T. Lin, Y. T. Tao, C. H. Chien, C. Tsai, *J. Mater. Chem.* **2005**, *15*, 2455–2463.
- [16] R. Hu, E. Lager, A. A. Aguilar, J. Liu, J. W. Y. Lam, H. H. Y. Sung, I. D. Williams, Y. Zhong, K. S. Wong, E. P. Cabrera, B. Z. Tang, *J. Phys. Chem. C* **2009**, *113*, 15845–15853.
- [17] a) G. Hua, Y. Li, A. M. Z. Slawin, J. D. Woollins, *Dalton Trans.* **2007**, 1477–1480; b) G. L. Ning, C. H. Liu, P. Qu, S. W. Zhang, Y. Lin, X. H. Zong, *Acta Chim. Sin.* **2000**, *58*, 1095–1098; c) Y. Q. Dong, J. W. Y. Lam, A. Qin, J. Liu, Z. Li, B. Z. Tang, J. Sun, H. S. Kwok, *Appl. Phys. Lett.* **2007**, *91*, 011111.
- [18] a) C. Lee, W. Yang, R. G. Parr, *Phys. Rev. B* **1988**, *37*, 785–789; b) A. D. Becke, *Phys. Rev. A* **1988**, *38*, 3098–3100; c) A. D. Becke, *J. Chem. Phys.* **1993**, *98*, 5648–5652.

Received: October 27, 2012

Revised: January 7, 2013

Published online: March 5, 2013